



ÉCOLE POLYTECHNIQUE
FÉDÉRALE DE LAUSANNE

Dispatch and clustering of ancillary services from distributed storage

Fabrizio Sossan
Distributed Electrical Systems Laboratory
Swiss Federal Institute of Technology of Lausanne, Switzerland

20th Power Systems Computation Conference - PSCC 2018
Dublin, 2018 June 11th

Outline

1. Mainstream trends for the integration of battery storage systems in electrical grids.
2. Dispatch of stochastic generation and distribution systems with batteries and downstream flexibility.
3. Practices for modelling and control of grid-connected battery systems in energy management applications.

1

Mainstream trends for the integration of battery storage systems in electrical grids.

Battery storage integration in the electrical grid

Two operational perspectives for the integration of batteries in the grid:

- Improving performance at the system level and increasing social benefit, e.g. reducing reserve, meeting reliability levels, reducing costs, relieving congestions in transmission systems, reducing CO₂ emissions (?)*.
- Enabling a larger installed capacity of distributed renewable generation in distribution systems (e.g. voltage control, congestion management, peak shaving).

* Storage might lead to increased CO₂ levels due to displacing gas in favor of coal generation, see e.g. [Lueken and Apt, 2014], [Preskill and Callaway, 2018].

Storage applications at the system level

“Classical” market-driven applications:

- Energy arbitrage: buying cheap electricity and reselling at higher price (economic advantage does not scale with the number of batteries).
- Reserve provision, i.e. use batteries to provide reserve capacity instead of conventional generation units.
- Primary frequency control.

Storage integration at system level – Tracking capability

AGC signal-tracking capability: coal-fired generation plant vs. battery [AEMO, 2018].

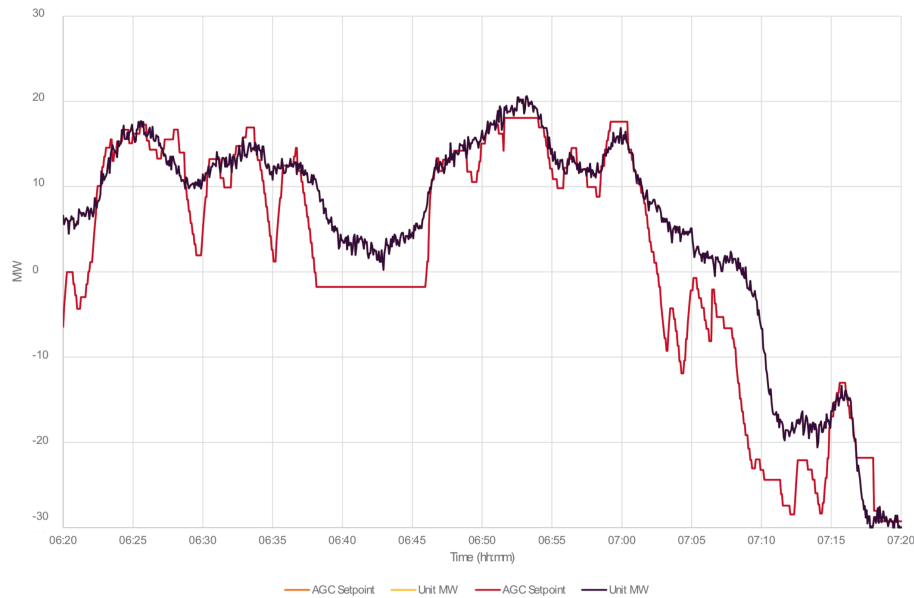


Fig.: Large coal power plant.

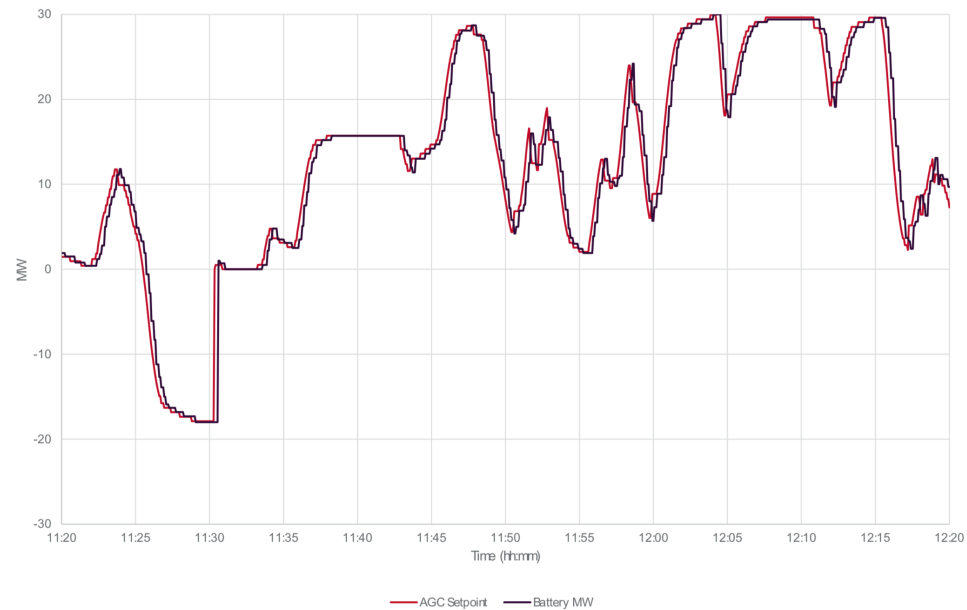


Fig.: *Hornsdale power reserve*
100/80 MW, 129 MWh grid-connected battery
(New South Wales, Australia, in operation since Dec 2017, connected to 275 kV HV).

Storage integration at system level – Empirical evidence

Ramping rate of *Hornsedale power reserve* during a contingency (18 Dec 2016, loss of 690 MW generating capacity) [AEMO, 2018]:

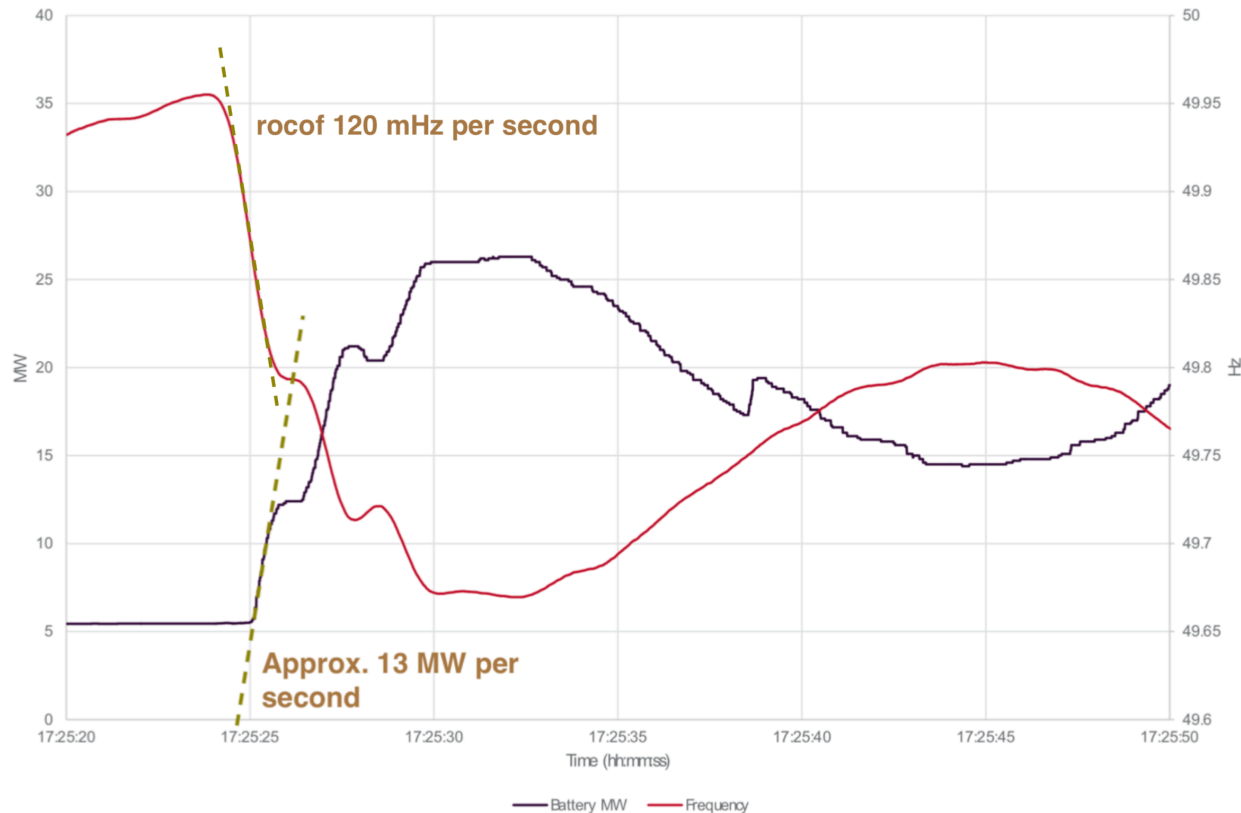


Fig.: *Hornsedale power reserve's* power delivery after a frequency drop. Estimated ramping rate is 13 MW/s, approx. 780% of nominal capacity per minute vs. 5, 15, 20% of coal, hydro, and gas.

Storage integration at system level – Empirical evidence, cont'd

2016 South Australia blackout. Grid with low meshing factor. 48% wind, 34% import, 18% gas. Faults on 5 transmission lines, 500 MW generation loss from wind farms due to storm conditions, activation of a loss-of-synchronism protection and tripping of 1 of the 2 line importing power.

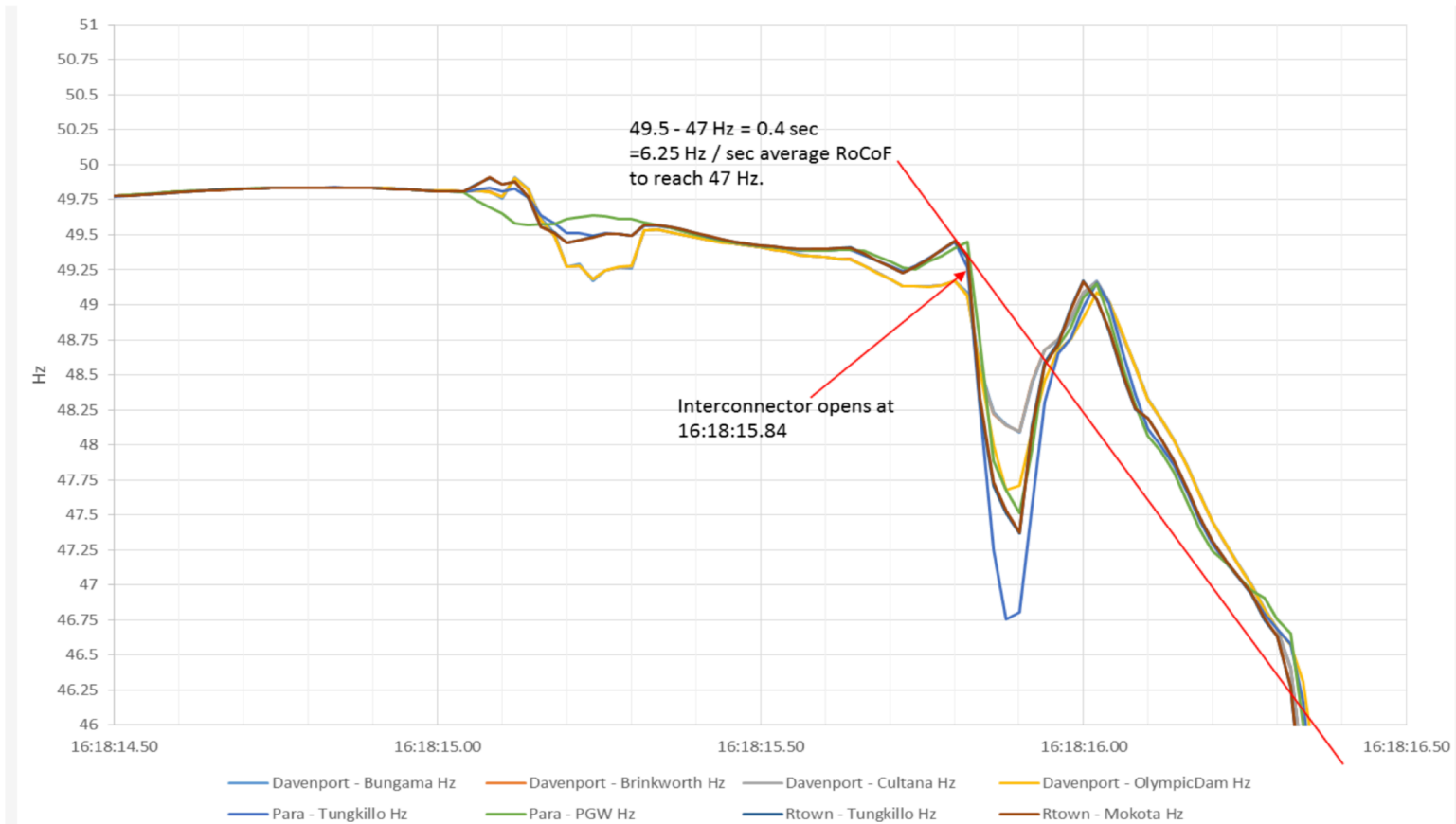


Fig.: Grid frequency before power blackout in South Australia on Sept. 26th [AEMO, 2017].

Applications of storage in distribution systems

Applications of storage in distribution systems have been proposed for:

- Peak-shaving, PV self-consumption.
- Mitigation of violations of nodal voltage and line current constraints, normally including a network model, where power flow equations are linearized (e.g. [Christakou et al., 2013], [Bolognani and Dorfler, 2015], [Bernstein and Dall'Anese, 2017], [Fortenbacher et al., 2017]) or convex relaxation (e.g. [Gan et al., 2015], [Nick et al., 2018]) to achieve tractable formulations.

Battery storage applications

General consensus on:

- operational value of distributed storage;
- delivering multiple services with batteries leads to better exploitation of storage capacity and shortens payback times;
- importance of storage will increase for increasing installed capacity of distributed generation (e.g. increased ramping duties of low-inertia power systems, grid control in LV/MV systems);
- specific policies and market regulations will play a crucial role in storage deployment.

2

Dispatch of stochastic generation and distribution systems with batteries and downstream flexibility.

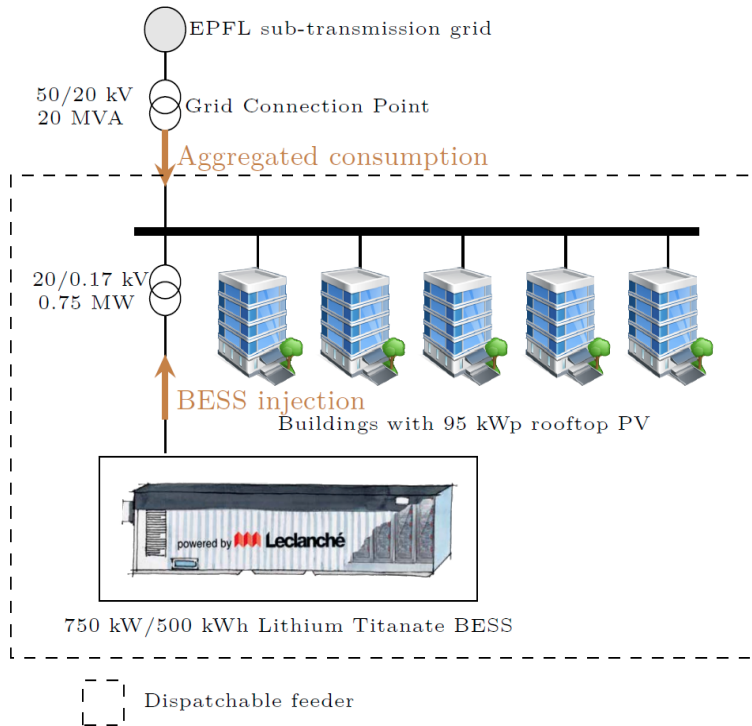
Dispatching stochastic resources

Dispatching stochastic resources, such as:

- PV plants [Marinelli et al., 2014], [Conte et al., 2017].
- wind farms [Abu Abdullah et al., 2015], and
- heterogeneous resources [Sossan et al., 2016], [Appino et al., 2018],

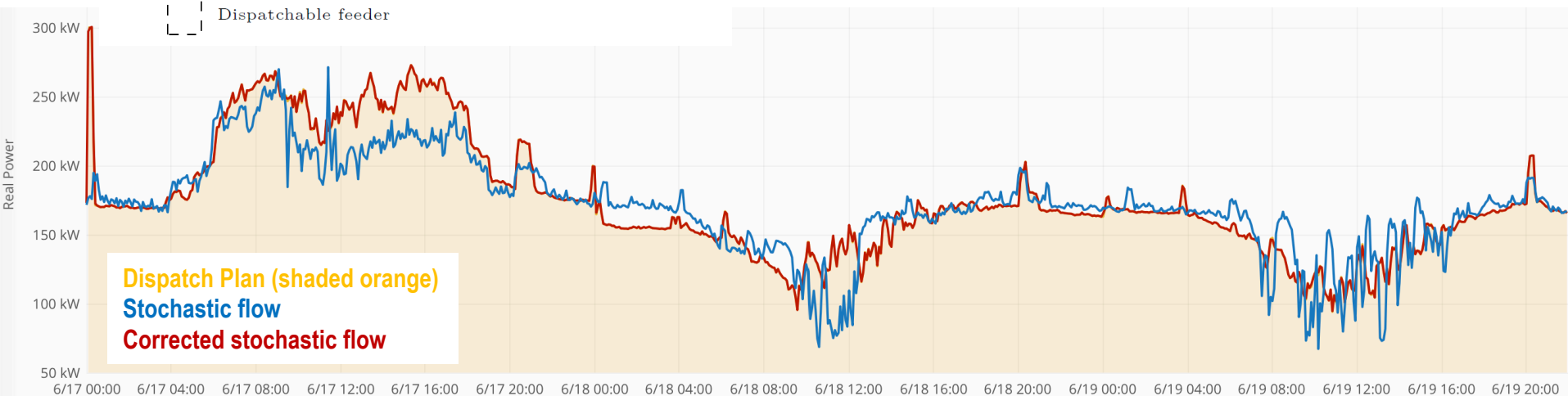
by leveraging forecasts and exploiting local flexibility is often advocated to reduce the amount of reserve requirements required to operate the grid.

Dispatching heterogeneous resources [Sossan et al., 2016]



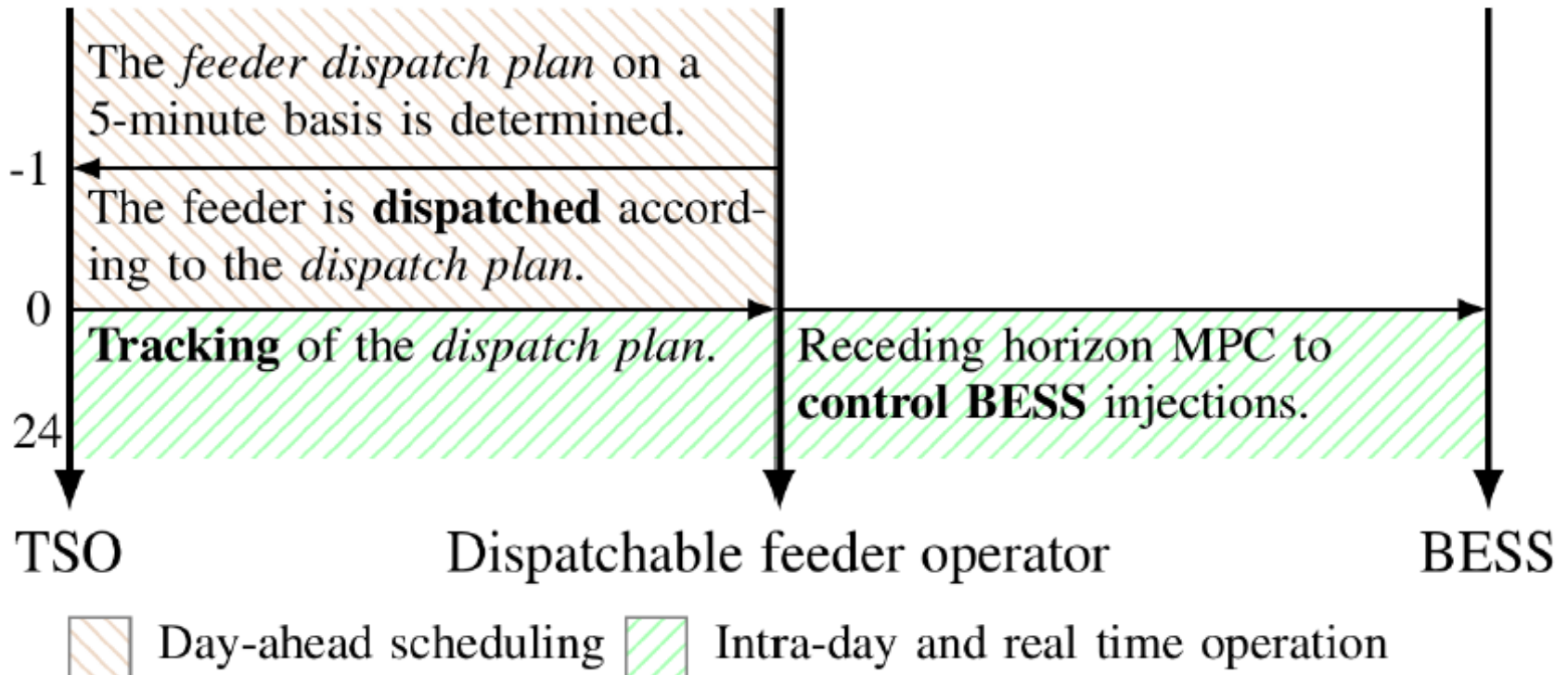
Problem Statement

- Compute a **dispatch plan** for a set of heterogeneous resources at the grid connection point (GCP) accounting for local grid constraints and local storage capacity (see also [Stai et al., 2017]).
- Control storage devices in real-time to track the dispatch plan.



Dispatch of stochastic resources – A two stage process

Time (hours before the beginning of the day of operation)



Dispatch of stochastic resources – Dispatch plan

The **dispatch plan** is a 1-day long sequence at 5 minute resolution of the scheduled power flow at the GCP:

$$\hat{P}_t = \hat{L}_t + F_t \quad t = 1, \dots, N$$

**Prosumption point
prediction at the GCP**

Offset profile

It restores an adequate battery state-of-energy to ensure that enough up/down-flexibility is available during operation to compensate for the mismatch between prosumption and realization.

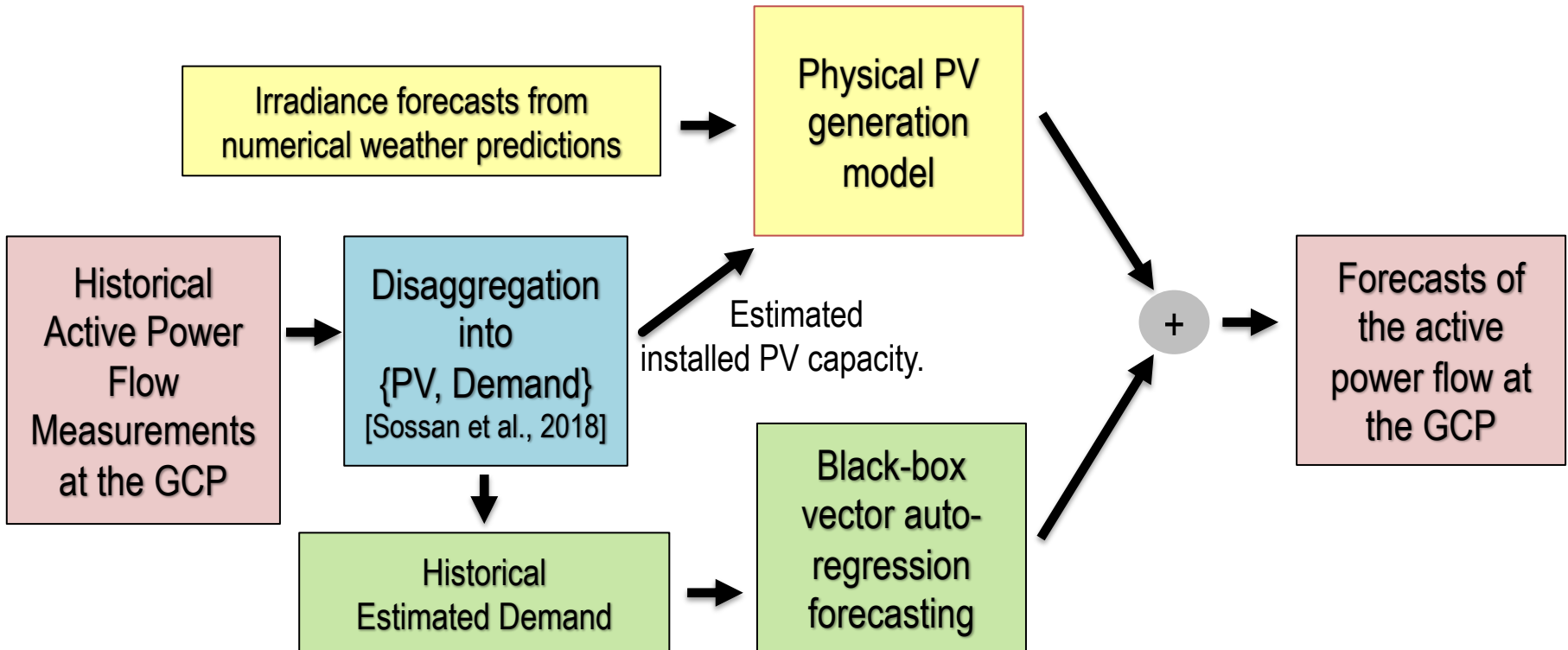
Dispatch of [..] resources – Day-ahead forecasts

$$\hat{P}_t = \hat{L}_t + F_t$$

Objective: forecasting the aggregated active power flow at the GCP of the set of heterogeneous resources for the next day.

Broad topic, generally. **Challenging and novel** due to the **low level of aggregation** (volatile series, very dependent on the mix of the underlying demand → whenever possible, tendency to adopt physical models to explain power flow patterns).

Procedure for hybrid black-box/physical forecasting with demand and PV:



Dispatch of stochastic resources – Offset profile

$$\hat{P}_t = \hat{L}_t + F_t$$

During operation, at time i , the battery compensates for the mismatch between the dispatch plan and the realization L_i . The battery's power injection is:

$$B_i = \hat{P}_i - L_i = F_i + \hat{L}_i - L_i$$

from the previous definition of the dispatch plan

Let $L_i^\uparrow, L_i^\downarrow$ the largest and smallest deviation of the prosumption's realization from its expected value (based on scenarios).

E.g., the battery's lowest injection at time i is

$$B_i^\downarrow = F_i + L_i^\downarrow$$

We seek for a solution $F = [F_1, \dots, F_N]$ so that the battery's state-of-energy and power injection are within limits.

$$F^o = \arg \min_{F \in \mathbb{R}^N} \left\{ \sum_{i=1}^N F_i^2 \right\}$$

Offset with least norm-2 (arbitrary standard choice, it could be just a feasibility problem)

subject to (for $i = 0, \dots, N - 1$):

$$F_i + L_i^\downarrow \geq B_{\min}$$

$$F_i + L_i^\uparrow \leq B_{\max}$$

Battery's injection within converter limit (only active power)

Worst case lowest state-of-energy must be higher than minimum allowed

$$\text{SOE}_{i+1}^\downarrow = \text{SOE}_i^\downarrow + \eta \left[F_i + L_i^\downarrow \right]^+ + 1/\eta \left[F_i + L_i^\downarrow \right]^-$$

$$\text{SOE}_{i+1}^\downarrow \geq \text{SOE}_{\min}$$

Charging efficiency

Worst case highest state-of-energy must be higher than minimum allowed

$$\text{SOE}_{i+1}^\uparrow = \text{SOE}_i^\uparrow + \eta \left[F_i + L_i^\uparrow \right]^+ + 1/\eta \left[F_i + L_i^\uparrow \right]^-$$

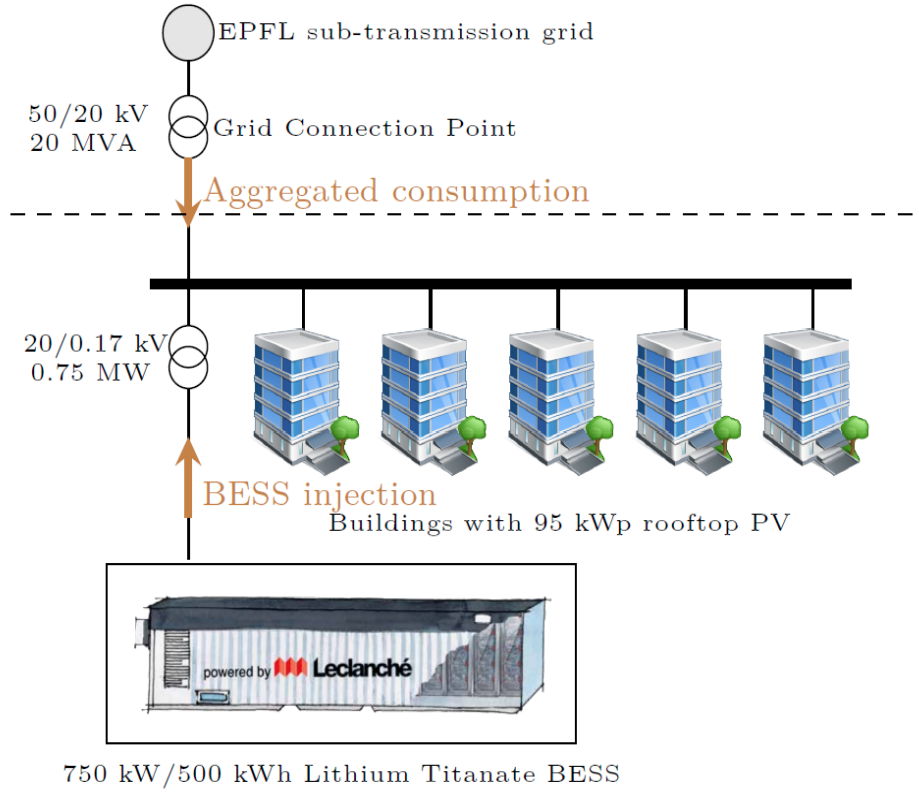
$$\text{SOE}_{i+1}^\uparrow \leq \text{SOE}_{\max}$$

$$\hat{P}_i \leq P_{\max}$$

Flow constraint at the GCP (assuming 1 pf)

(nonconvex due to the sign operators, convexified in [Sossan et al., 2016])

Experimental validation: setup at EPFL, CH



Dispatchable feeder

- Single measurement point at the GCP.
- 350 kW peak demand during winter.
- 95 kWp roof-top PV installation.

Experimental validation: results

Dispatched operation -- 14 Jan 2016

<https://snapshot.raintank.io/dashboard/snapshot/PuW1Rf5d470Q0gsT7UNponM25bGDNTRA>

Dispatched operation -- 13 Jan 2016

<https://snapshot.raintank.io/dashboard/snapshot/cDS4IDniZjRiePXvusnmQXOmMwpGLnR6>

Dispatched operation + Peak Shaving -- 22/06/2016

<https://snapshot.raintank.io/dashboard/snapshot/LSF3bPxtWYDjHVu6siEr1VPb92EXNkd6>

Dispatched Operation + Load Levelling -- 14/03/2016

<https://snapshot.raintank.io/dashboard/snapshot/4ztn800czpAzEFRzbG0mWc1A2pKeC9ab>

Dispatched operation (continuous operation) -- 16 to 19/03/2016

<https://snapshot.raintank.io/dashboard/snapshot/TNbEgP7j1AWhaW7cEK1ZiK3tY1Or7P4U>

Provision of multiple ancillary services with same battery

Single service applications lead to poor exploitation of battery's power and energy ratings.

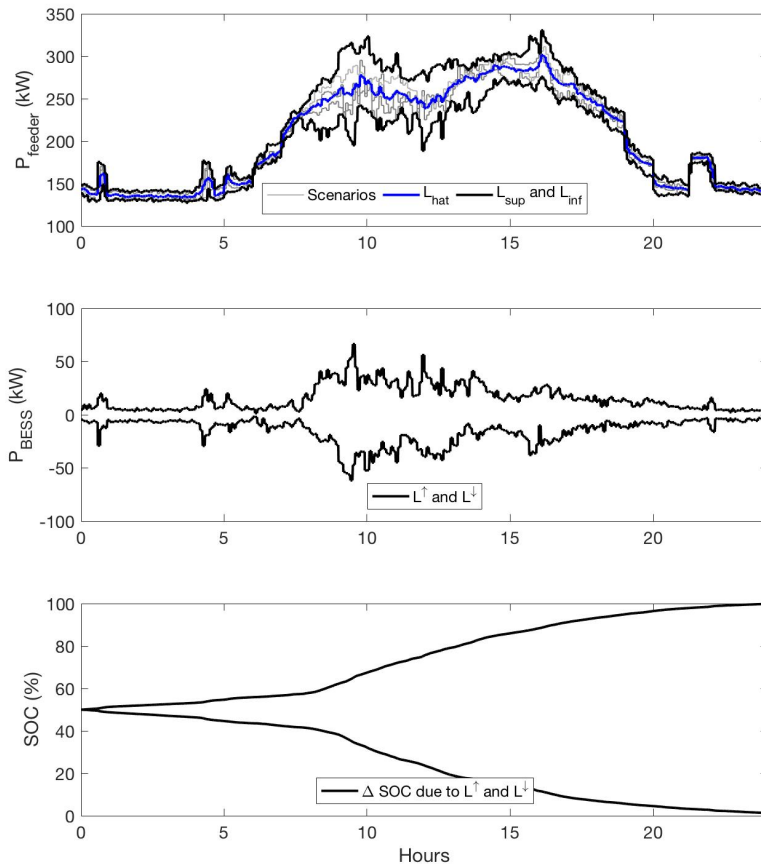


Fig.: Dispatch planning with **higher** uncertainty.

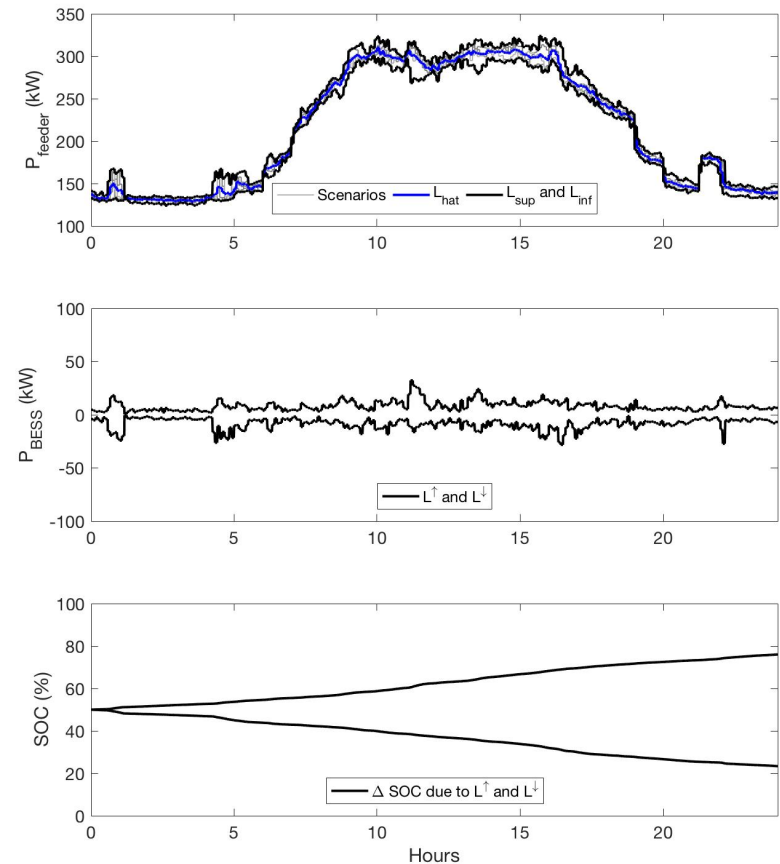


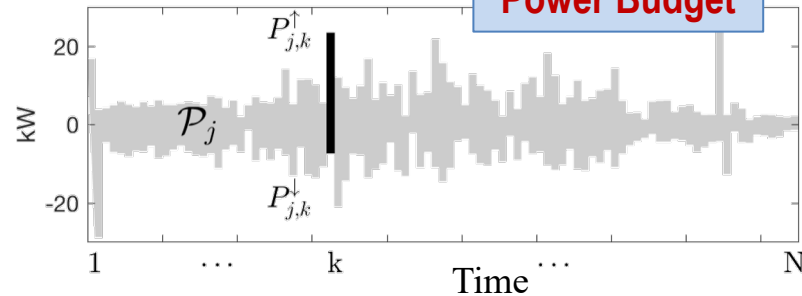
Fig.: Dispatch planning with **lower** uncertainty.

Residual power/energy capacity can be used to **provide multiple ancillary services simultaneously.**

Stacking of ancillary services [Namor et al., 2018]

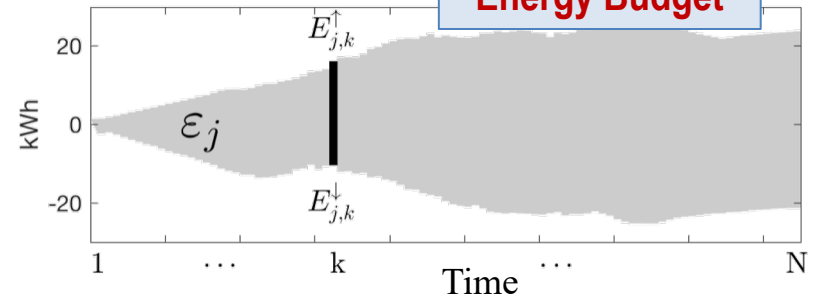
We have multiple services to provide. We define for each grid ancillary service j the:

Power Budget



$$\mathcal{P}_j = \left\{ \left[P_{j,k}^{\downarrow}(x, \theta), P_{j,k}^{\uparrow}(x, \theta) \right], k = 1, \dots, N \right\}$$

Energy Budget



$$\mathcal{E}_j = \left\{ \left[E_{j,k}^{\downarrow}(x, \theta), E_{j,k}^{\uparrow}(x, \theta) \right], k = 1, \dots, N \right\}$$

parametrized over vector of controller's parameters x and forecast of the unitary budgets θ .

Operator to determine width of envelopes: $w(\mathcal{E}_j(x, \theta)) \triangleq \{ E_{j,k}^{\uparrow}(x, \theta) - E_{j,k}^{\downarrow}(x, \theta), k = 1, \dots, N \}$

We seek to find the controllers' parameters which maximize the exploitation of the battery energy capacity subject to the battery's power and energy constraints.

$$\arg \max_x \left\| w \left(\sum_j \mathcal{E}_j(x, \theta) \right) \right\|_1$$

subject to:

$$E_{init} + \sum_j \mathcal{E}_j(x, \theta) \in [E_{min}, E_{max}]$$

$$\sum_j \mathcal{P}_j(x, \theta) \in [-P_{max}, P_{max}]$$

Stacking of ancillary services: Results [Namor et al., 2018]

Dispatch + primary frequency regulation (PFR)

	Dispatch	PFR
Power Budget	Worst case high and worst case low power deviation from the dispatch plan.	Drop coefficient (unknown, to determine) time worst case frequency deviation (200 mHz).
Energy Budget	Integral of worst case deviations.	5-95% quantiles of the distribution of the accumulated frequency deviation in 1 day over a 2-year period.

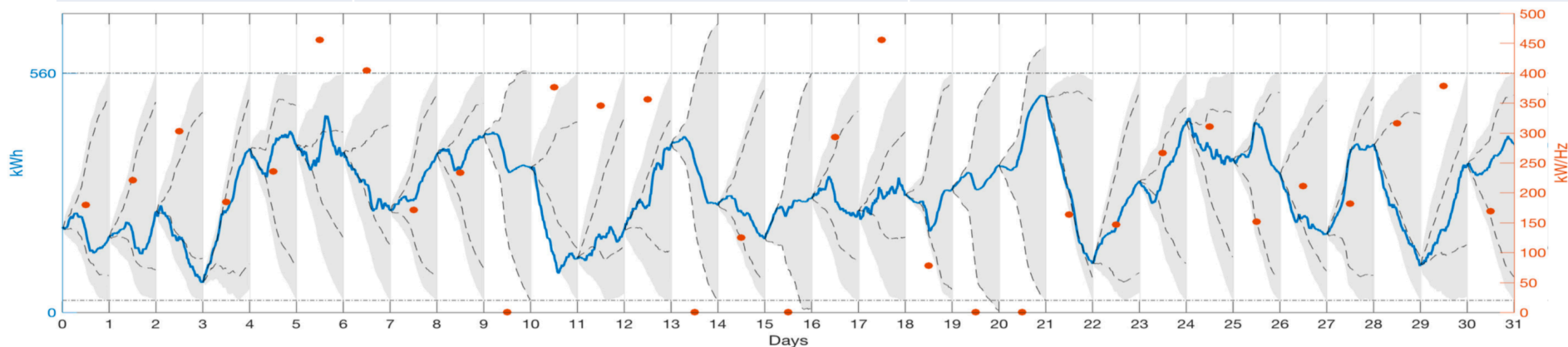


Fig.: Battery's state of energy (SOE): realization (**thick blue line**), worse cases for dispatch (**dashed black line**), worse cases for dispatch + PFR (**shaded grey**), and allocated drop coefficient (**orange dots**).

[Link to results](#)

Dispatch: extension to multiple controllable resources

With multiple flexible element in the mix (e.g. **battery** + building with controllable **electric space heating**), the problem can be extended by (in brief):

- Compute one dispatch plan per each element in the mix [Fabietti et al., 2018].
- The aggregated dispatch plan is the algebraic sum of the individuals dispatch plans.
- The real-time control problem with multiple controllable elements is distributable (tractable) [Fabietti et al., 2017] [Gupta et al., 2018].

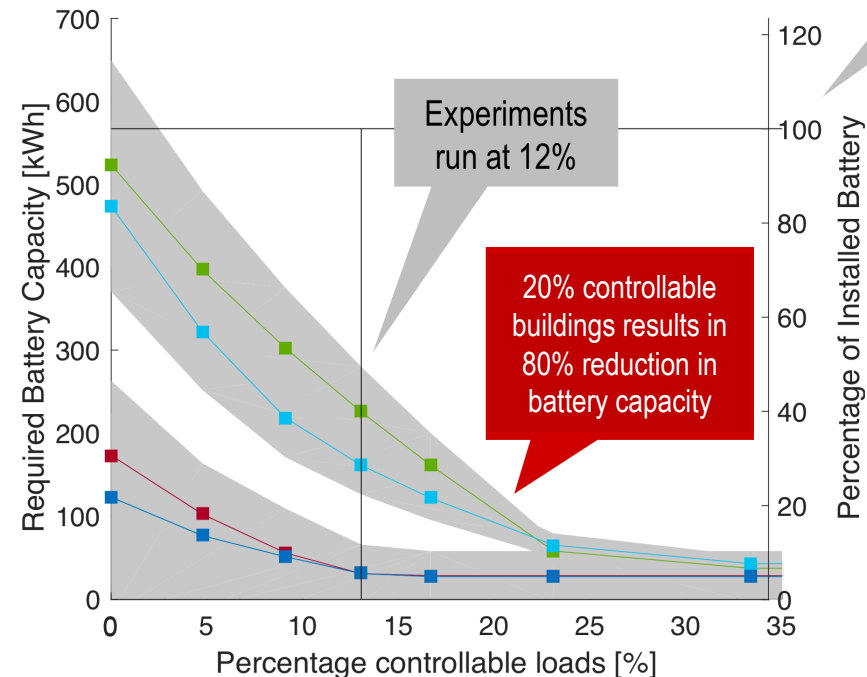


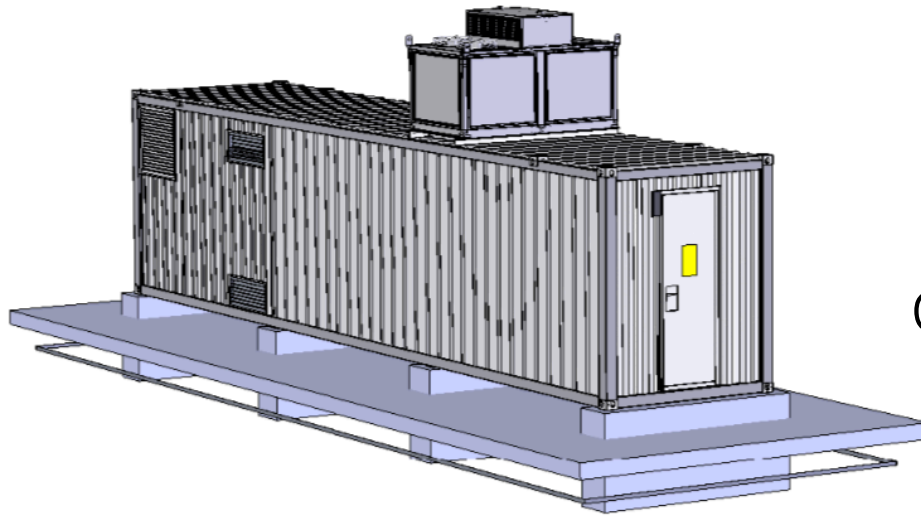
Fig.: Dispatch with batteries and flexible demand. Battery capacity to achieve control targets decreases for larger penetration of controllable loads [Fabietti et al., 2017].

3

Practices for modelling and control of grid-connected battery systems in energy management applications.

Anatomy of a grid-connected battery system

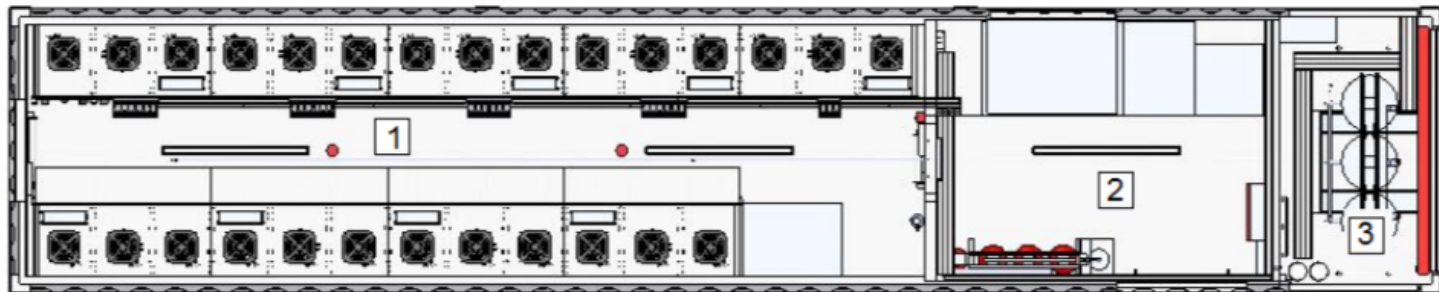
720 kVA, 560 kWh battery system



Container, 12 x 3 x 2 m, approx. 20 tons

Air conditioning (7 kW) and ventilation system (0.5 kW)

Fire extinguishing system



Battery stack

DC/AC Power Converter

Step-up transformer

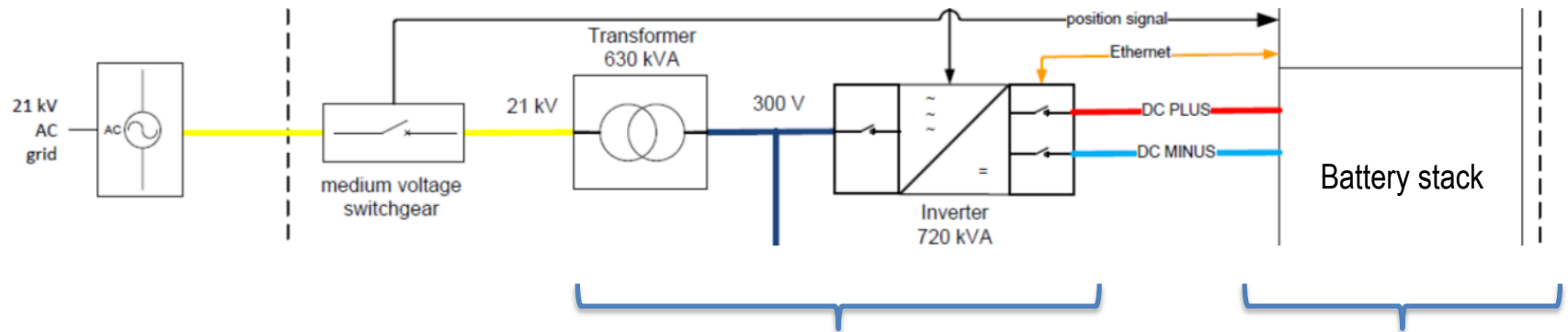
Courtesy of *Leclanché*.

Example of utility-scale grid-connected battery

Parameter	Value
Nominal Capacity	720 kVA/560 kWh
GCP Voltage	20 kV
DC Bus Voltage Range	600/800 V
Cell Technology (Anode/Cathode)	Lithium Titanate Oxide (LTO) Nichel Cobalt Alumnum Oxide (NCA)
Number of racks	9 in parallel
Number of modules per rack	15 in series
Cells configuration per module	20s3p
Total number of cells	8100
Cell nominal voltage	2.3 V (limits 1.7 to 2.7 V)
Cell nominal capacity	30 Ah (69 Wh)
Round-trip efficiency (AC side)	94-96%
Round-trip efficiency (DC side)	97-99%



Grid-connected batteries: modelling requirements



Models discussed in the next section, with focus on time constants for energy management applications:

Converter

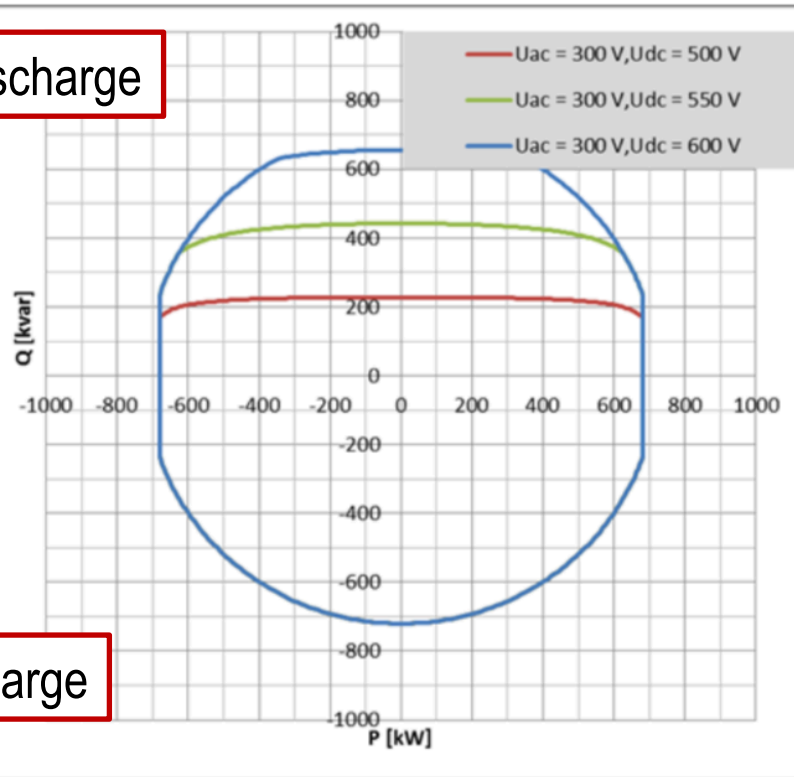
Lumped model of the cells' stack

Fig.: Components of a grid-connected battery energy storage systems.

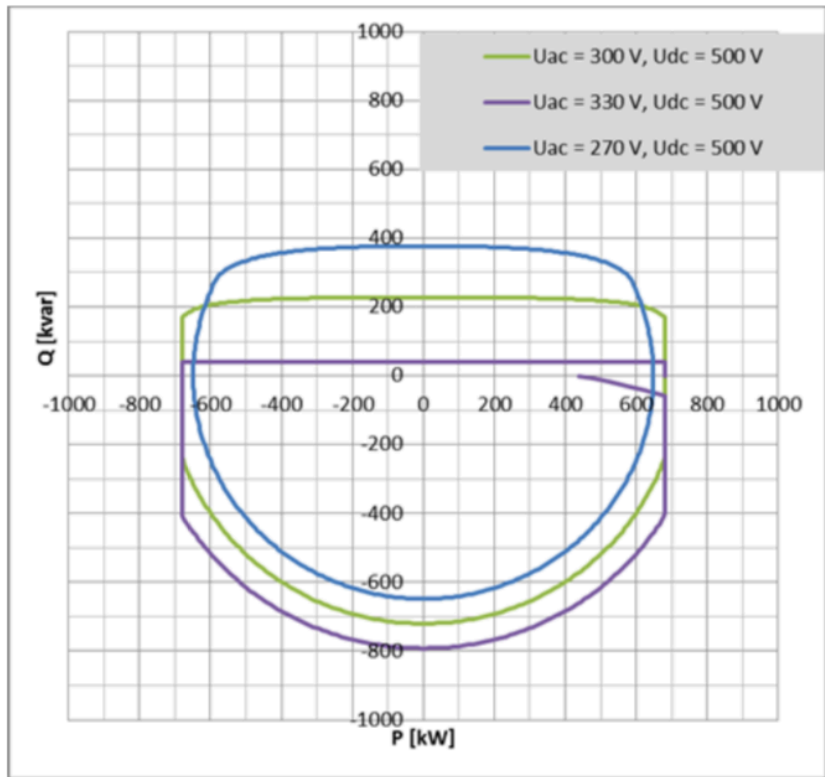
Modelling for energy management – Power converter

Converter's real capability curves (or PQ characteristics):

Discharge



Charge



Voltage constant on grid side (U_{ac}),
variable on DC bus (U_{dc})

Voltage constant on DC bus (U_{dc}),
variable on grid side (U_{ac})

Converter's capability modelled with a static circular PQ characteristic (convex), piecewise linearized, see e.g. [Nick et al., 2014]. Converter + transformer losses modelled with a constant coefficient (fraction of cell stack's losses).

Modelling the Battery's state of charge (SOC)

1. Integral of the power over the energy capacity (brutal, especially for inefficient storage).

$$\text{SOC}_{t+1} = \text{SOC}_t + \frac{1}{T} \frac{1}{E_{\text{nom}}} P_t$$

2. Constant efficiency. It can be rendered convex by expressing the power as the sum of 2 mutually exclusive (to be verified a-posteriori!) variables [Kraning et al., 2011]:

$$\text{SOC}_{t+1} = \text{SOC}_t + \frac{1}{T} \frac{1}{E_{\text{nom}}} \left(\eta [P_t]^+ - \frac{1}{\eta} [P_t]^- \right)$$

3. When the problem is coupled to a load flow, the battery's series resistance is a new line in an augmented load flow [Stai et al., 2017] (little additional complexity!).
4. Second order model to capture rate capacity effect or charge relaxation effect, see e.g. application in [Fortenbacher et al., 2017].

Modelling requirements – Battery's voltage dynamics

Two time constant (TTC) models widely adopted to describe **lumped** voltage dynamics on the DC bus as a function of the DC current.

Pros	Cons
<p>Capture dynamics quite accurately.</p> <p>Tractable (linear).</p> <p>Few parameters to identify.</p> <p>It can be estimated from measurements.</p> <p>Easy to apply (one variable to observe).</p>	<p>Parameters depend on:</p> <ul style="list-style-type: none">• State of charge• Charge/Discharge rate• Temperature <p>Gives no insight into underlying electrochemical processes.</p> <p>Fails to capture ageing mechanism.</p>

Data-driven identification of TTC models

Steps:

1. Perform experiments with pseudo random binary signal (PRBS) and collect voltage and current measurements on the DC bus.
2. Model formulation.
3. Parameter identification.
4. Validation (and cross-validation).
5. If performance is not acceptable. Change model and repeat.

See e.g. [Namor et al., 2018b].

Data-driven identification of TTC models – PRBS

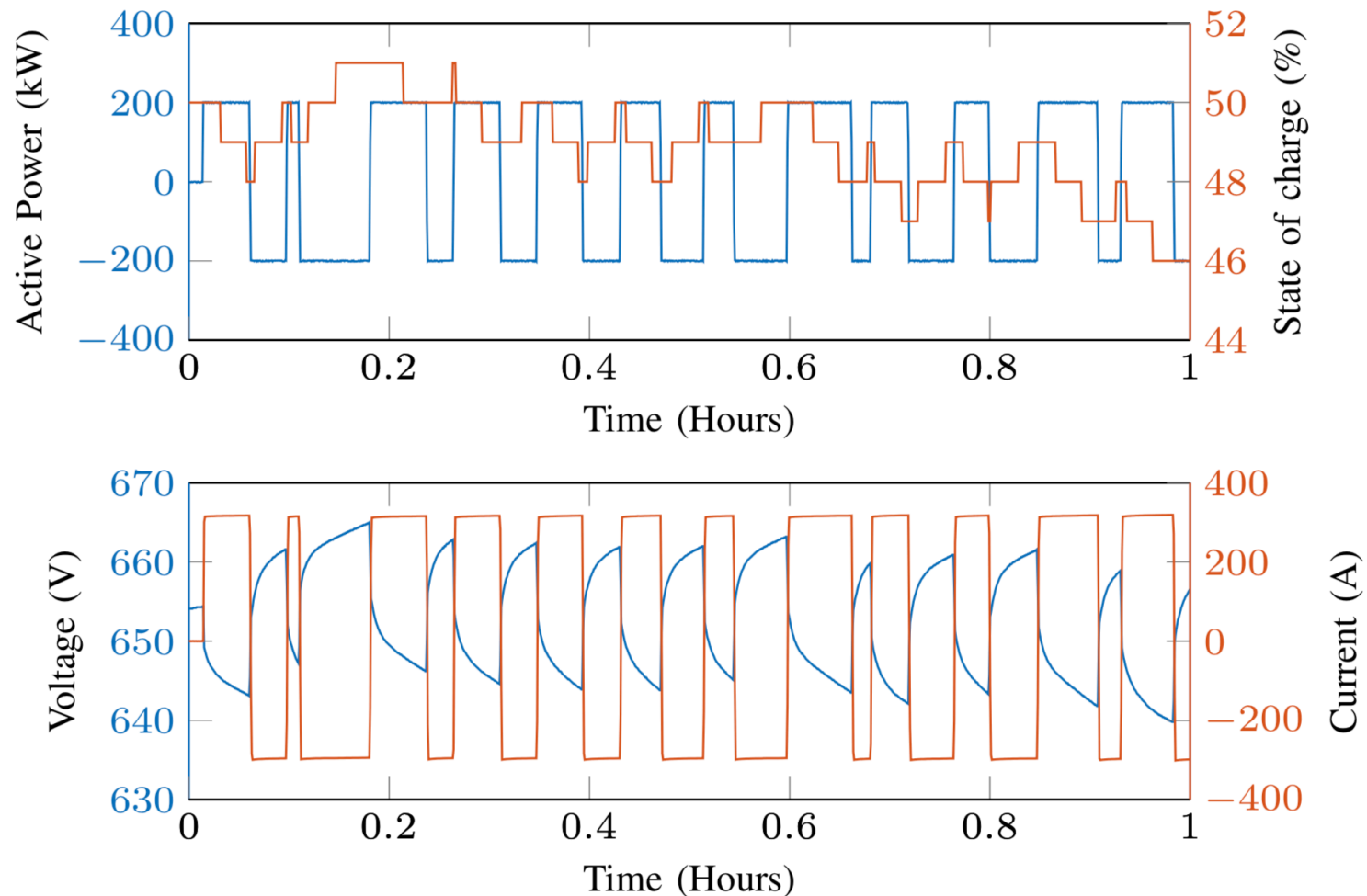
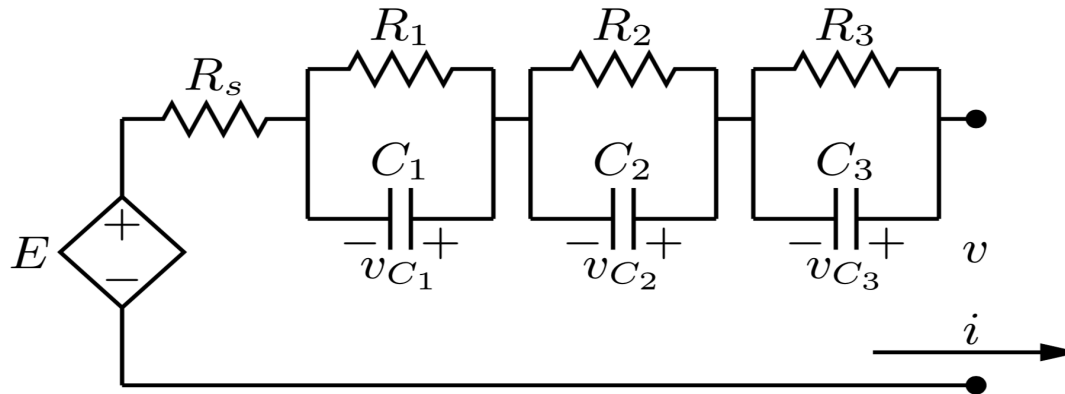


Fig.: Example of zero-mean PRBS signal.

Identification of TTC models – Model formulation



3rd state normally needed to capture time dynamics in the scale of few seconds.

2 or 3 states vs 1 output. State estimation required to apply the model in practice.

Fig.: Three time constant model with parameters $R_x C_x$ and $E = \alpha + \beta z$.

Stochastic state-space model:

$$dx = \mathcal{A}_c(\theta)xdt + \mathcal{B}_c(\theta)u(t)dt + \mathcal{K}_c(\theta)dw$$

$$v_k = \mathcal{C}x_k + \mathcal{D}(\theta)u_k + \mathcal{G}(\theta)g_k,$$

State vector and input (for two time constants,

the additional state is the battery's state-of-charge).

$$x = [v_{C_1} \quad v_{C_2} \quad z]^T$$

$$u_{tk} = [i_{tk} \quad 1]^T.$$

State-space matrices:

$$\mathcal{A}_c = -\text{diag}\left(\frac{1}{R_1 C_1}, \frac{1}{R_2 C_2}, 0\right)$$

$$\mathcal{B}_c = \begin{bmatrix} \frac{1}{C_1} & 0 \\ \frac{1}{C_2} & 0 \\ \frac{1}{Q} & 0 \end{bmatrix}$$

$$\mathcal{K}_c = \text{diag}(k_1, k_2, k_3)$$

$$\mathcal{C} = [1 \quad 1 \quad \beta]$$

$$\mathcal{D} = [R_s \quad \alpha]$$

$$\mathcal{G} = \sigma_g.$$

Identification of TTC models – Model validation

Residual analysis

One-step ahead prediction error: $e_{k|k-1} = \hat{v}_{k|k-1} - v_k$

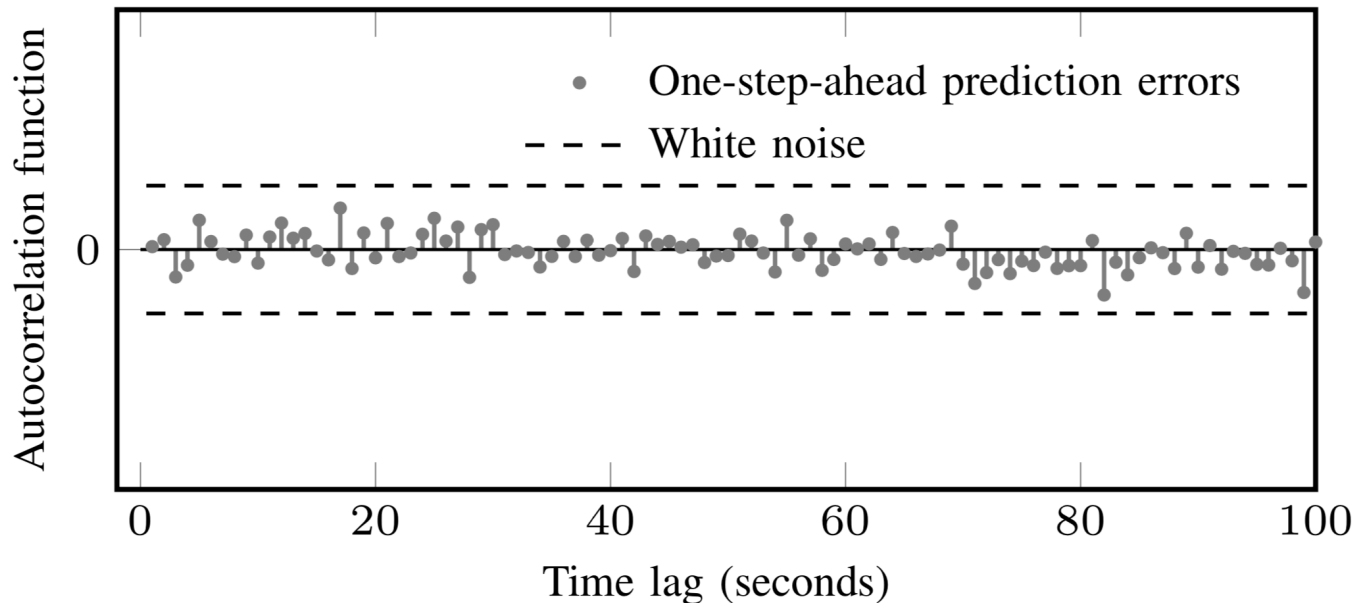


Fig.: Autocorrelation of the one-step ahead prediction errors vs white noise to check residual structure in the series.

Example: energy model predictive control (MPC) of a battery

Let e_k be the energy throughput's set-point for a battery. The problem is determining a power trajectory to achieve e_k while respecting battery's voltage and current constraints. [Sossan et al., 2016].

Two possible decision variables:

- Battery's power output. Linear (integral) objective, nonlinear and nonconvex current and voltage constraints.
- Battery's current. Linear voltage and current constraints, cost function

$$\left(E_{\bar{k}|k}(\mathbf{i}_{\bar{k}|k}) - e_k \right)^2.$$

Battery energy throughput as a function of the battery DC current (convex under certain conditions see next)

Set-point

in the form $b(g(x))$, convex if $g(x)$ is convex and b convex non-decreasing, thus nonconvex. Convex formulation.

Energy MPC – Battery’s energy is quadratic in the current

The battery’s energy throughput is the sum over time of the battery’s power output, i.e. product of battery’s DC current, DC voltage and converter efficiency alpha:

$$E_{\bar{k}|k}(\cdot) = \alpha \mathbf{v}_{\bar{k}|k}^T \mathbf{i}_{\bar{k}|k}$$

Battery AC energy throughput

Battery DC voltage sequence

Battery DC current sequence

Battery’s DC voltage as a function of the current is from the linear TTC model:

$$\mathbf{v}_{\bar{k}|k} = \phi^v \mathbf{x}_k + \psi_i^v \mathbf{i}_{\bar{k}|k} + \psi_1^v \mathbf{1}$$

Battery system state (Kalman-estimated)

Phi, gamma from battery state-space matrices

Replacing the second into the first yields:

$$E_{\bar{k}|k}(\cdot) = \alpha \left(\mathbf{x}_k^T \phi^{vT} \mathbf{i}_{\bar{k}|k} + \mathbf{i}_{\bar{k}|k}^T \psi_i^{vT} \mathbf{i}_{\bar{k}|k} + \mathbf{1}^T \psi_1^{vT} \mathbf{i}_{\bar{k}|k} \right)$$

i.e., sum of two linear terms and a quadratic term in the current. Convex if ψ is SDP.

Energy MPC for a battery – A convex formulation

We use the previous result to formulate a convex problem of the energy tracking point. It maximizes the current (i.e. linear cost function) subject to the energy throughput being less or equal to the target energy throughput e_k (i.e. convex inequality).

$$\mathbf{i}_{\bar{k}|k}^o = \arg \max_{\mathbf{i} \in \mathbb{R}^{(k-\bar{k}+1)}} \left\{ \mathbf{1}^T \mathbf{i}_{\bar{k}|k} \right\}$$

subject to :

$$\alpha \left(x_k^T \phi^{vT} \mathbf{i}_{\bar{k}|k} + \mathbf{i}_{N|t}^T \psi_i^{vT} \mathbf{i}_{\bar{k}|k} + \mathbf{1}^T \psi_r^{vT} \mathbf{i}_{\bar{k}|k} \right) \leq e_k \quad (\text{BESS energy throughput, convex if } \psi_i^v \text{ is SDP})$$

$$\mathbf{1} \cdot i_{\min} \preceq \mathbf{i}_{\bar{k}|k} \preceq \mathbf{1} \cdot i_{\max} \quad (\text{Current constraints})$$

$$\mathbf{1} \cdot \Delta_{i,\min} \preceq H \mathbf{i}_{\bar{k}|k} \preceq \mathbf{1} \cdot \Delta_{i,\max} \quad (\text{Current ramping constraints})$$

$$\mathbf{v}_{\bar{k}|k} = \phi^v v_k + \psi_i^v \mathbf{i}_{\bar{k}|k} + \psi_1^v \mathbf{1} \quad (\text{Voltage model})$$

$$\mathbf{1} \cdot v_{\min} \preceq \mathbf{v}_{\bar{k}|k} \preceq \mathbf{1} \cdot v_{\max} \quad (\text{Voltage constraints})$$

$$\mathbf{SOC}_{\bar{k}|k} = \phi^{\text{SOC}} \text{SOC}_k + \psi_i^{\text{SOC}} \mathbf{i}_{\bar{k}|k} \quad (\text{SOC model})$$

$$\mathbf{1} \cdot \text{SOC}_{\min} \preceq \mathbf{SOC}_{\bar{k}|k} \preceq \mathbf{1} \cdot \text{SOC}_{\max} \quad (\text{SOC constraints})$$

Energy MPC for a battery – Experimental results

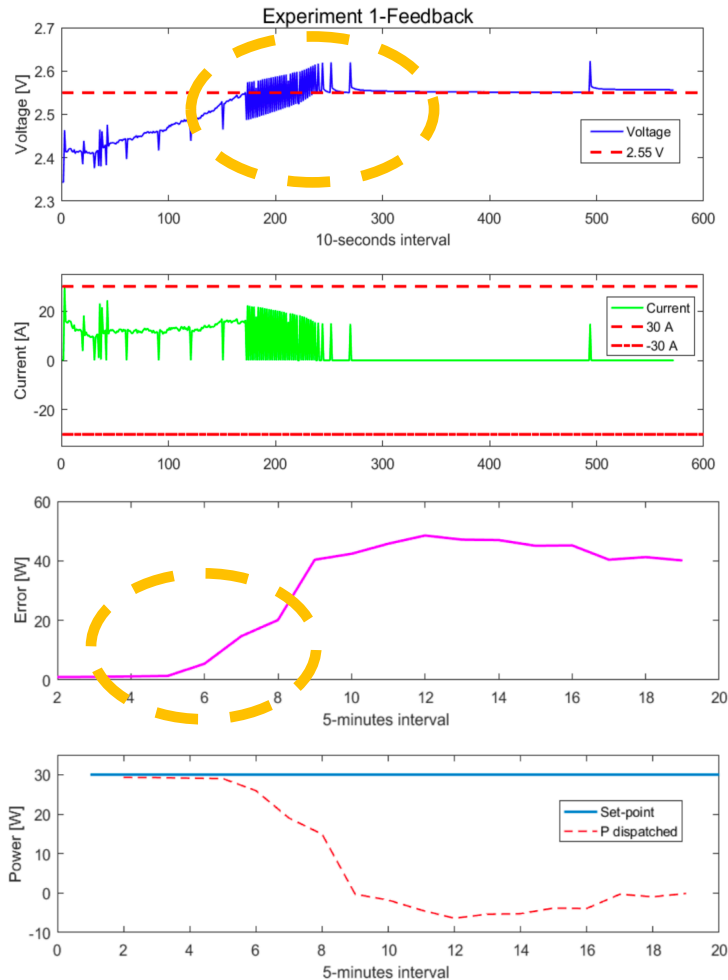


Fig.: Single battery cell with integral feedback control loop. Voltage constraints violations.

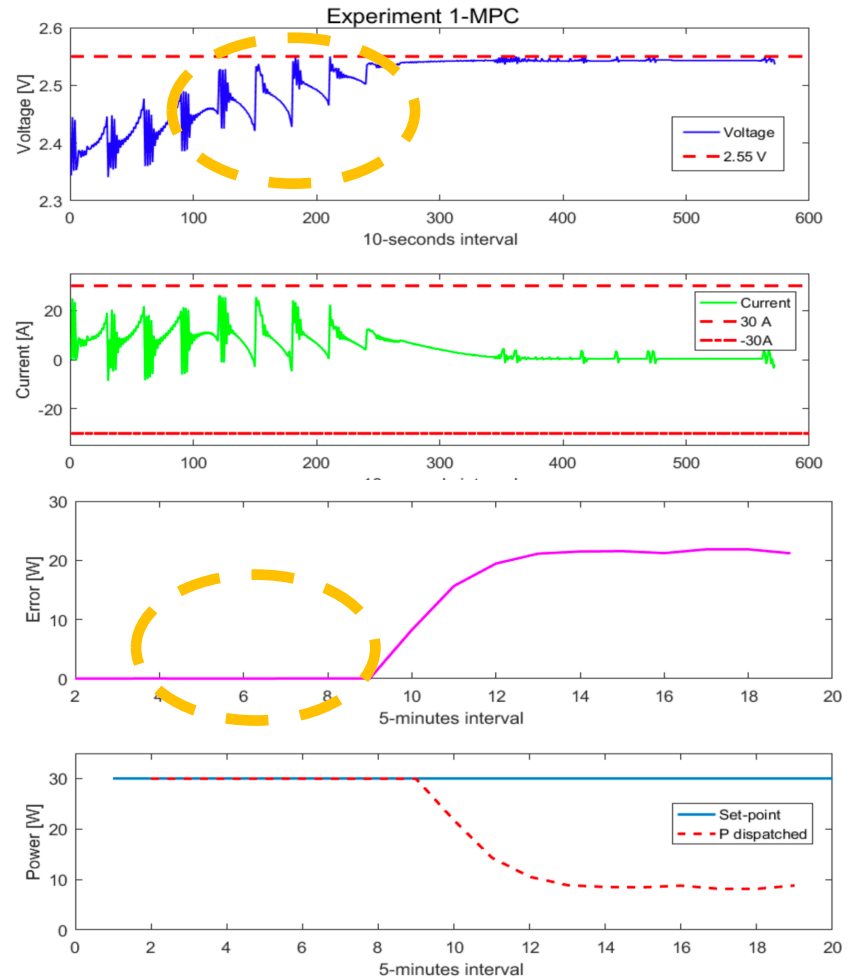


Fig.: Single battery cell with energy MPC. Better tracking performance with no violations.

A side note about ageing and ageing-aware control

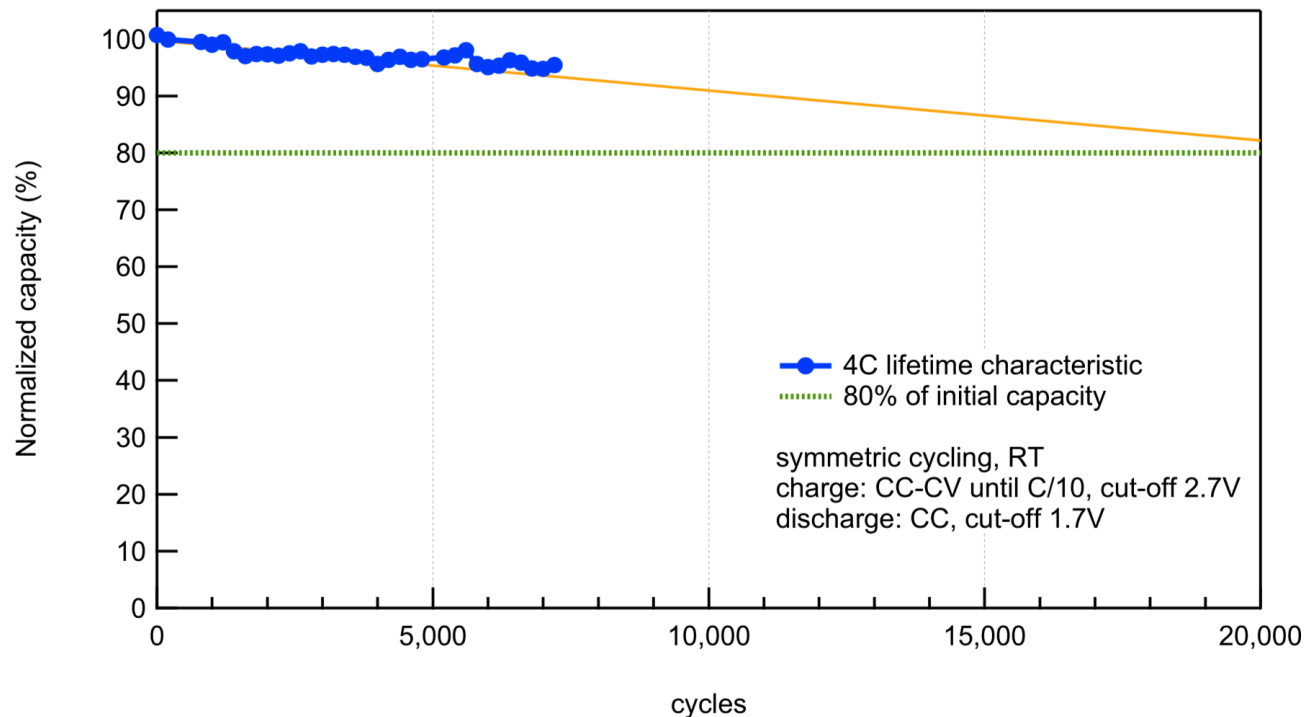


Fig.: Empirical assessment of battery ageing of a LTO cell based on laboratory tests. Courtesy of *Leclanché*.

Rule-of-thumb estimates (wo including path dependent aging):

- Expected life due to cycling: **55 years at 1 cycle per day**
- Expected calendar life: **15 years**



Ageing-aware control policies should be designed according to the available technology.

Summary

1. Integration of battery storage in electrical grids. Two perspectives: increasing the performance at the system level, and enabling safe integration of renewable energies in distribution systems.
2. A framework to dispatch heterogeneous resources as a control paradigm for controlling battery systems and downstream flexibility → towards self-dispatching distribution systems?
3. Anatomy of a real-life grid-connected battery storage system – mainstream modelling practices for power converters, battery voltage dynamics, and state-of-charge.

References

- [Abu Abdullah et al., 2015] Abu Abdullah, M., Muttaqi, K., Sutanto, D., and Agalgaonkar, A. (2015). An effective power dispatch control strategy to improve generation schedulability and supply reliability of a wind farm using a battery energy storage system. *Sustainable Energy, IEEE Transactions on*, 6.
- [AEMO, 2017] AEMO (2017). Black system south Australia 28 september 2016. Technical report, Australian Energy Market Operator.
- [AEMO, 2018] AEMO (2018). Initial operation of the Hornsdale power reserve battery energy storage system. Technical report, Australian Energy Market Operator.
- [Appino et al., 2018] Appino, R. R., Angel Gonzalez Ordiano, J., Mikut, R., Faulwasser, T., and Hagenmeyer, V. (2018). On the use of probabilistic forecasts in scheduling of renewable energy sources coupled to storages. *Applied Energy*, 210:1207 – 1218.
- [Bernstein and Dall’Anese, 2017] Bernstein, A. and Dall’Anese, E. (2017). Linear power-flow models in multiphase distribution networks. In *2017 IEEE PES Innovative Smart Grid Technologies Conference Europe (ISGT-Europe)*, pages 1–6.
- [Bolognani and Dorfler, 2015] Bolognani, S. and Dorfler, F. (2015). Fast power system analysis via implicit linearization of the power flow manifold. In *2015 53rd Annual Allerton Conference on Communication, Control, and Computing (Allerton)*, pages 402–409.
- [Byrne and Silva-Monroy, 2012] Byrne, R. H. and Silva-Monroy, C. A. (2012). Estimating the maximum potential revenue for grid connected electricity storage: Arbitrage and regulation. Sandia National Laboratories.
- [Christakou et al., 2013] Christakou, K., LeBoudec, J.-Y., Paolone, M., and Tomozei, D.-C. (2013). Efficient computation of sensitivity coefficients of node voltages and line currents in unbalanced radial electrical distribution networks. *IEEE Transactions on Smart Grid*, 4(2).
- [Conte et al., 2017] Conte, F., Massucco, S., Saviozzi, M., and Silvestro, F. (2017). A stochastic optimization method for planning and real-time control of integrated pv-storage systems: Design and experimental validation. *IEEE Transactions on Sustainable Energy*, pages 1–1.
- [Fabietti et al., 2017] Fabietti, L., Gorecki, T. T., Namor, E., Sossan, F., Paolone, M., and Jones, C. N. (2017). Dispatching active distribution networks through electrochemical storage systems and demand side management. In *1st IEEE Conference on Control Technology and Applications*.
- [Fabietti et al., 2018] Fabietti, L., Gorecki, T. T., Namor, E., Sossan, F., Paolone, M., and Jones, C. N. (2018). Enhancing the dispatchability of distribution networks through electric energy storage systems and flexible demand: Control architecture and experimental validation. *Elsevier Energy and Buildings*, Accepted for Publication.
- [Fortenbacher et al., 2017] Fortenbacher, P., Mathieu, J. L., and Andersson, G. (2017). Modeling and optimal operation of distributed battery storage in low voltage grids. *IEEE Transactions on Power Systems*, 32(6):4340–4350.
- [Gan et al., 2015] Gan, L., Li, N., Topcu, U., and Low, S. H. (2015). Exact convex relaxation of optimal power flow in radial networks. *IEEE Transactions on Automatic Control*, 60(1):72–87.
- [Gupta et al., 2018] Gupta, R., Sossan, F., Scolari, E., Namor, E., Fabietti, L., Jones, C., and Paolone, M. (2018). An ADMM-based coordination and control strategy for PV and storage to dispatch stochastic prosumers: Theory and experimental validation. *PSCC2018*.

References – cont'd

- [Kazemi et al., 2017] Kazemi, M., Zareipour, H., Amjady, N., Rosehart, W. D., and Ehsan, M. (2017). Operation scheduling of battery storage systems in joint energy and ancillary services markets. *IEEE Transactions on Sustainable Energy*, 8(4):1726–1735.
- [Koller et al., 2015] Koller, M., Borsche, T., Ulbig, A., and Andersson, G. (2015). Review of grid applications with the Zurich 1MW battery energy storage system. *Electric Power Systems Research*, 120:128 – 135. *Smart Grids: World’s Actual Implementations*.
- [Kraning et al., 2011] Kraning, M., Wang, Y., Akuiyibo, E., and Boyd, S. (2011). Operation and configuration of a storage portfolio via convex optimization. In *Proceedings of the 18th IFAC World Congress*, volume 18, pages 10487–10492.
- [Lueken and Apt, 2014] Lueken, R. and Apt, J. (2014). The effects of bulk electricity storage on the PJM market. *Energy Systems*, 5(4):677–704.
- [Marinelli et al., 2014] Marinelli, M., Sossan, F., Costanzo, G. T., and Bindner, H. W. (2014). Testing of a predictive control strategy for balancing renewable sources in a microgrid. *IEEE Transactions on Sustainable Energy*.
- [Namor et al., 2017] Namor, E., Sossan, F., Cherkaoui, R., and Paolone, M. (2017). Battery storage system optimal exploitation through physics-based model predictive control. In *PowerTech, 2017 IEEE Manchester*.
- [Namor et al., 2018] Namor, E., Sossan, F., Cherkaoui, R., and Paolone, M. (2018). Control of battery storage systems for the simultaneous provision of multiple services. *IEEE Transactions on Smart Grid*, pages 1–1.
- [Namor et al., 2018b] Namor, E., Sossan, F., Scolari, E., Cherkaoui, R., and Paolone, M. (2018b). Experimental assessment of the prediction performance of dynamic equivalent circuit models of grid-connected battery energy storage systems. In *IEEE International Conference on Innovative Smart Grid Technologies (ISGT)*.
- [Nick et al., 2018] Nick, M., Cherkaoui, R., Boudec, J. Y. L., and Paolone, M. (2018). An exact convex formulation of the optimal power flow in radial distribution networks including transverse components. *IEEE Transactions on Automatic Control*, 63(3):682–697.
- [Nick et al., 2014] Nick, M., Cherkaoui, R., and Paolone, M. (2014). Optimal allocation of dispersed energy storage systems in active distribution networks for energy balance and grid support. *IEEE Transactions on Power Systems*, 29(5):2300–2310.
- [Preskill and Callaway, 2018] Preskill, A. and Callaway, D. (2018). How much energy storage do modern power systems need? *arXiv preprint arXiv:1805.05115*.
- [Sossan et al., 2016] Sossan, F., Namor, E., Cherkaoui, R., and Paolone, M. (2016). Achieving the dispatchability of distribution feeders through prosumers data driven forecasting and model predictive control of electrochemical storage. *IEEE Transactions on Sustainable Energy*, 7(4).
- [Sossan, 2017] Sossan, F. (2017). Equivalent electricity storage capacity of domestic thermostatically controlled loads. *Energy*, 122.
- [Sossan et al., 2018] Sossan, F., Nespoli, L., Medici, V., and Paolone, M. (2018). Unsupervised disaggregation of photovoltaic production from composite power flow measurements of heterogeneous prosumers. *IEEE Transactions on Industrial Informatics*.
- [Stai et al., 2017] Stai, E., Reyes-Chamorro, L., Sossan, F., Boudec, J. Y. L., and Paolone, M. (2017). Dispatching stochastic heterogeneous resources accounting for grid and battery losses. *IEEE Transactions on Smart Grid*, pages 1–1.